

Acoustic-phonon-based interaction between coplanar quantum circuits in a magnetic field

M. G. Prokudina,¹ V. S. Khrapai,¹ S. Ludwig,² J. P. Kotthaus,² H. P. Tranitz,³ and W. Wegscheider⁴

¹*Institute of Solid State Physics, Russian Academy of Sciences, 142432 Chernogolovka, Russian Federation*

²*Center for NanoScience and Department für Physik, Ludwig-Maximilians-Universität, Geschwister-Scholl-Platz 1, D-80539 München, Germany*

³*Institut für Experimentelle und Angewandte Physik, Universität Regensburg, D-93040 Regensburg, Germany*

⁴*Solid State Physics Laboratory, ETH Zurich, 8093 Zurich, Switzerland*

(Received 5 August 2010; revised manuscript received 14 October 2010; published 16 November 2010)

We explore the acoustic-phonon-based interaction between two neighboring coplanar circuits containing semiconductor quantum point contacts in a perpendicular magnetic field B . In a drag-type experiment, a current flowing in one of the circuits (unbiased) is measured in response to an external current in the other. In moderate B the sign of the induced current is determined solely by the polarity of B . This indicates that the spatial regions where the phonon emission/reabsorption is efficient are controlled by magnetic field. The results are interpreted in terms of nonequilibrium transport via skipping orbits in a two-dimensional electron system.

DOI: 10.1103/PhysRevB.82.201310

PACS number(s): 73.23.-b

Nonequilibrium behavior in coupled nanocircuits in solid-state devices is often studied in drag-type experiments. That is, an external current is sent through one (drive) circuit and a current (or voltage) induced is measured in a second neighboring (detector) circuit. Different interaction mechanisms include Coulomb drag,^{1,2} exchange of ultrahigh-frequency photons³⁻⁵ or other energy quanta,⁶ rectification,⁷ and coulombic or phononic backaction.⁸⁻¹⁰

A typical size of a lateral nanostructure defined in a GaAs-based two-dimensional electron system (2DES) is on the order of $1\ \mu\text{m}$. In comparison, the nanostructure transport current probes a distribution function of carriers in the 2DES leads on a length scale of at least $10\ \mu\text{m}$ (elastic mean-free path or a longer relevant length scale). It is tempting to interpret the drag-type experiments in such nanostructures in terms of purely one- or zero-dimensional physics. However, the surrounding leads can sometimes play a key role, as it is the case for an acoustic-phonon-based interaction between the two nanocircuits.^{6,8,9,11,12} One way to verify the importance of the leads is to apply a small perpendicular magnetic field (B), which modifies charge transport in 2DESs thanks to a Lorentz force. At the same time, the impact of small B on nanostructures can often be reduced to a trivial magnetic-subbands depopulation, as, e.g., in a quantum point contact (QPC).¹³ Application of $B > 1\text{ T}$ was relevant in Refs. 2 and 4 however the role played by the 2DES leads in those experiments have not been carefully analyzed.

In this Rapid Communication, we investigate the influence of B on the acoustic-phonon-based interaction between the leads of two coplanar isolated QPCs in a drag-type experiment. At $B=0$ the counterflow effect in such a system has been recently observed,¹¹ with currents in the drive circuit (I_{DRIVE}) and detector circuit (I_{DET}) flowing in the opposite directions. We find that in moderate B the direction of I_{DET} is insensitive to that of I_{DRIVE} and, instead, determined solely by the polarity of B . This is interpreted in terms of a nonequilibrium skipping orbits transport along the edges of the 2DESs. Our observations (i) demonstrate that the role played by the leads can be decisive in drag-type experiments in magnetic field and (ii) provide a possible way to verify its importance.

Our samples are prepared on a GaAs/AlGaAs heterostuc-

ture containing a 2DES 90 nm below the surface with an electron density of $2.8 \times 10^{11}\text{ cm}^{-2}$ and a low-temperature mobility of $1.4 \times 10^6\text{ cm}^2/\text{Vs}$. For each of the two samples, a number of metallic gates is deposited with e-beam lithography on the surface of the crystal, as shown in Figs. 1(a) and 1(b). Applying a negative voltage on the central gate (C), one creates two electrically isolated circuits, separated by a distance of several hundreds of nanometers. In each circuit, a QPC is defined via negative biasing a metallic gate on a corresponding side of the gate C. An external dc bias voltage, V_{DRIVE} , is applied to one lead of the drive QPC while its second lead is grounded. A current I_{DET} generated in the circuit of the detector QPC is measured with a home-made I - V converter (conversion ratio 10^{-9} A/V) connected to one of its leads. The other lead of the detector QPC is kept at an input offset potential of the I - V converter ($< 10\ \mu\text{V}$), to maintain the detector circuit unbiased. In both circuits, a

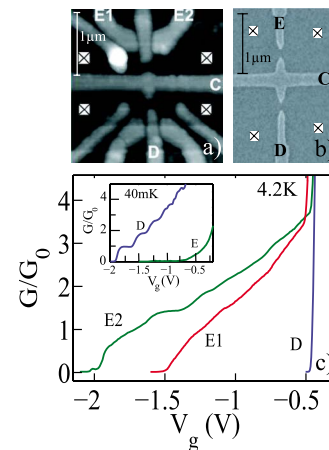


FIG. 1. (Color online) (a) Atomic-force micrograph of the split-gate nanostructure on the surface of sample 1. (b) Scanning electron micrograph of the nanostructure equivalent to that of sample 2. E, E1, E2, and D, respectively, denote the gates used for the definition of the drive QPC and detector QPC; crosses denote ohmic contacts. (c) Normalized conductance of the QPCs as a function of their gate voltages for sample 1 (body) and 2 (inset) at respective bath temperatures.

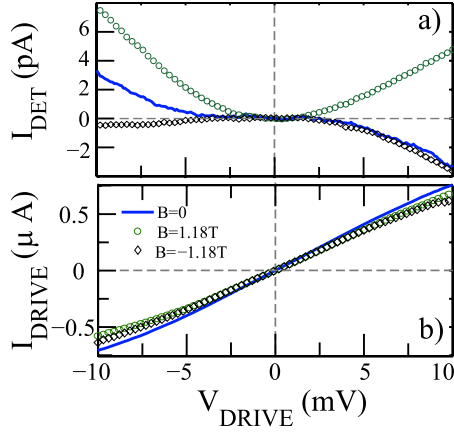


FIG. 2. (Color online) Results for sample 1 at 4.2 K. (a) Detector current at $B=0$ (solid line) and in moderate magnetic fields (symbols, same legend as in panel b) as a function of drive bias. (b) I - V curves of the drive QPC taken simultaneously with the data in (a).

positive sign of the current is chosen for electrons flowing to the left. Our results were obtained with both ac and dc measurements. For ac measurements, V_{DRIVE} was modulated with a small voltage of 100 μV at frequencies in the range 7–33 Hz. The real phase ac component of I_{DET} was measured with a lock in. The experiments were performed in a liquid ^4He cryostat at a temperature of 4.2 K (sample 1) and a $^3\text{He}/^4\text{He}$ dilution refrigerator at a base temperature of 40 mK (sample 2). Exchanging either detector and drive circuit or the bias and ground leads of the drive QPC yields qualitatively the same results. This is also true if in sample 1 either gate E1 or E2 are used to define the drive QPC (data given below are obtained with E2). The origin of the measured detector signals is only consistent with the acoustic-phonon-based interaction. The corresponding discussion of Refs. 6 and 11 takes into account the interaction bandwidth, the strongly nonlinear response, the insensitivity to physical distance between the QPCs and the conservation laws. Apparent unimportance of a two orders of magnitude temperature variation as well as B dependencies observed here also fit into the phononic scenario.

Figure 1(c) displays linear-response conductance for each of the QPCs used in our experiments. The conductance is zero at low gate voltages (QPC pinched-off) and goes up with increasing gate voltage. A clear conductance quantization is visible only for one of the QPCs studied (D for sample 2), whereas a poor quality of others and/or high-temperature (for sample 1) prevent its observation. Note, though, that the key ingredient for thermoelectriclike effects is the energy dependence of the detector QPC transparency,^{7,11} rather than the conductance quantization. Throughout the Rapid Communication, the detector QPC is kept near the pinch-off with resistance $\sim 10^2$ k Ω . The drive QPC is either (i) relatively open or (ii) nearly pinched-off. The serial resistance of the ohmic contacts is negligible in all cases except for the open drive QPC regime in sample 2. In the last case, the voltage drop corresponding to $B=0$ resistance of the ohmic contacts was subtracted from V_{DRIVE} . First, we concentrate on the open drive QPC regime with $R_{\text{DRIVE}} \sim 10$ k Ω .

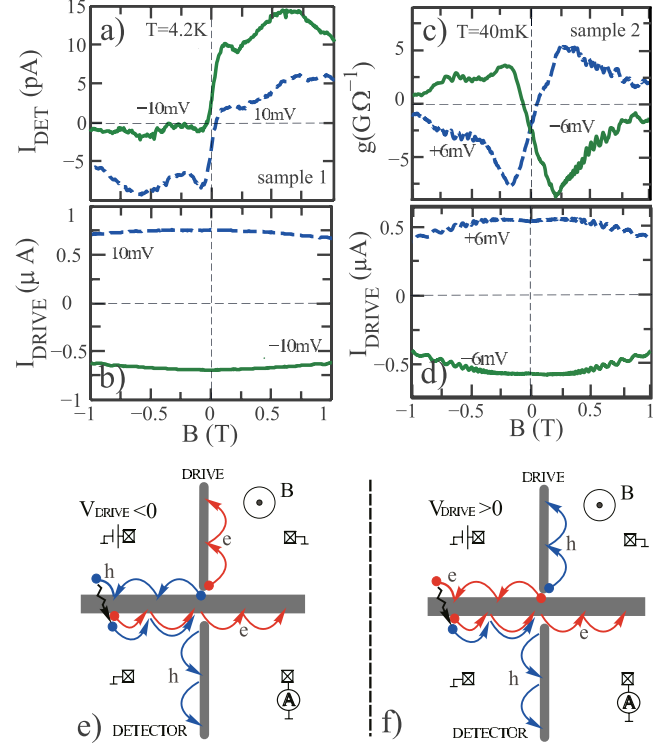


FIG. 3. (Color online) Open regime with $R_{\text{DRIVE}} \sim 10$ k Ω . (a) Detector and (b) drive currents at fixed $V_{\text{DRIVE}} = \pm 10$ mV as a function of magnetic field $-1 \text{ T} \leq B \leq 1 \text{ T}$ for sample 1. [(c) and (d)] Derivative g of the (c) detector signal and (d) drive current at fixed $V_{\text{DRIVE}} = \pm 6$ mV as a function of magnetic field $-1 \text{ T} \leq B \leq 1 \text{ T}$ for sample 2. [(e) and (f)] Quasiclassical trajectories of nonequilibrium carriers skipping along the electrostatic edges of the 2DES nearby the drive QPC and detector QPC. Sketches are drawn for $B < 0$ and $V_{\text{DRIVE}} < 0 / > 0$ (e)/(f). Arrows indicate the direction of electrons group velocity near the edge. Schematics of the measurement connections is also shown, with ohmic contacts represented by crossed squares.

At $B=0$ we reproduce previous results obtained on a different sample.¹¹ The current induced in the detector QPC at $B=0$ is shown in Fig. 2(a) as a function of V_{DRIVE} by a solid line (sample 1). I_{DET} is a thresholdlike function of V_{DRIVE} , changing its sign on reversal of V_{DRIVE} . For $V_{\text{DRIVE}} \gtrsim 3$ mV a finite I_{DET} is observed, directed opposite to I_{DRIVE} (referred to as a counterflow effect in Ref. 11). In relatively high $|B| \sim 1$ T applied perpendicular to the 2DES the situation is changed dramatically. The sign of I_{DET} is independent of that of I_{DRIVE} (symbols in Fig. 2). Instead, it is determined by the sign of B ($B > 0$ corresponds to magnetic field pointing downward into the crystal). Below we refer to this regime as a B -driven regime. At the same time, no effect of B is seen in the drive QPC I - V curve, apart from a minor increase in its resistance [Fig. 2(b)]. The absolute value of I_{DET} in magnetic field depends on the polarity of V_{DRIVE} [Fig. 2(a)], which is discussed below.

In Fig. 3(a) we show how the detector current evolves as a function of B in sample 1 at fixed $V_{\text{DRIVE}} = \pm 10$ mV. A transition to the B -driven regime occurs at small fields. Here, I_{DET} steeply increases, linear in B and changes the sign when B is swept from -0.1 to $+0.1$ T. Outside this interval, in the

B -driven regime, no strong B -dependence is observed. The same qualitative behavior is found in sample 2 with a differential ac measurement. In Fig. 3(c) the measured derivative $g \equiv dI_{\text{DET}}/dV_{\text{DRIVE}}$ is plotted for $V_{\text{DRIVE}} = \pm 6$ mV. Note that, e.g., a positive I_{DET} at a negative V_{DRIVE} results in $g < 0$. At $B=0$ the counterflow effect is again reproduced with $g < 0$ regardless the sign of V_{DRIVE} . With increasing $|B|$ a transition to the B -driven behavior occurs in Fig. 3(c), which manifests itself as a sign change in g in response to V_{DRIVE} reversal. As seen from Figs. 3(b) and 3(d), for both samples, the simultaneously measured I_{DRIVE} is a featureless weakly parabolic function of B with a small oscillatory contribution associated with the Shubnikov-de Haas effect at low temperature [Fig. 3(d)].

At $B=0$, the counterflow effect has been explained in a thermoelectric analogy.¹¹ The associated spatial asymmetry of the energy flow from the drive circuit occurs in the non-linear regime and is determined by the direction of the current I_{DRIVE} . The thermoelectric analogy is also applicable to the B -driven regime, where the direction of the I_{DRIVE} is irrelevant to that of the I_{DET} . The origin of the asymmetry in this case is related to a cyclotron motion of charge carriers in perpendicular magnetic fields. In a quasiclassical picture, bulk 2D electrons circle around cyclotron orbits of a radius $R_C \propto |B|^{-1}$ thanks to the Lorentz force. In sufficiently high B , such that $R_C < L$, where $L \approx 11 \mu\text{m}$ is the elastic mean-free path set by a disorder in our samples, the electrons trajectories are localized within regions of size smaller than L . This is not the case for carriers incident on or leaving from a QPC, whose cyclotron circles cross the electrostatic edge of the 2DES. These carriers exhibit a specular reflection at the edge and follow skipping-orbit trajectories.

In Figs. 3(e) and 3(f) the motion of nonequilibrium carriers next to the QPCs is sketched for $B < 0$ and different signs of V_{DRIVE} . Here, e and h stand for nonequilibrium electrons above and nonequilibrium holes (i.e., unoccupied electron states) below the Fermi energy, respectively. In the (upper) drive circuit the nonequilibrium e and h exit on different sides of the drive QPC, as determined by the sign of V_{DRIVE} . In the vicinity of the constriction, the carriers in the drive circuit follow two quasiclassical trajectories skipping along the respective edges of the 2DES electrostatically defined by the split gates. One of them skips along the (horizontal) gate C and the other along the (vertical) drive QPC gate. The nonequilibrium carriers moving along the gate C (e/h for $V_{\text{DRIVE}} > 0 / < 0$) are most efficient in transferring energy to the adjacent lead of the detector circuit [zigzag arrows in Figs. 3(e) and 3(f)]. As discussed in Ref. 9, such energy transfer is likely to be mediated by acoustic phonons which are reabsorbed in the detector within $\sim 1 \mu\text{m}$. As a result, nonequilibrium e - h pairs are excited in the detector, moving along the edge toward the detector QPC. Note, that nonequilibrium population of the skipping-orbit states can also occur indirectly, via excitation of e and h in the bulk 2DES, with their subsequent diffusion to the edge. On the average, more nonequilibrium electrons traverse the detector QPC, because of the energy dependence of the QPC transparency,¹¹ which results in the measured I_{DET} . As follows from Figs. 3(e) and 3(f), $I_{\text{DET}} < 0$ for $B < 0$, independent of the direction of I_{DRIVE} . Similar sketches would be obtained for $B > 0$ via mir-

roring about the vertical axis and simultaneously changing the sign of V_{DRIVE} , which explains the detector current reversal: $I_{\text{DET}} > 0$ for $B > 0$.

The reversal of V_{DRIVE} corresponds to changing the type of nonequilibrium carriers skipping along the gate C in the drive circuit [compare Figs. 3(e) and 3(f)]. The fraction of the total energy (later dissipated in the leads as Joule heat) injected with e in one lead of the drive QPC is higher than the fraction injected with h in the other lead. This comes from the positive-energy dependence of the QPC transparency.¹¹ In the B -driven regime, this e - h asymmetry manifests itself as a higher absolute value of I_{DET} and g for the e sign of V_{DRIVE} [a slight V_{DRIVE} asymmetry of the total Joule heat inferred from Figs. 3(b) and 3(d) has a minor effect here]. Correspondingly, in Figs. 3(a) and 3(c) we find the detector response stronger for $V_{\text{DRIVE}} > 0 (< 0)$ at $B < 0 (> 0)$. This behavior is more pronounced in sample 1 [Fig. 3(a)], which is likely caused by a stronger energy dependence of the drive QPC transparency in this case.

The regions of the 2DESs where emission/reabsorption of the acoustic phonons is efficient are different in the counterflow regime ($B=0$) and in the B -driven regime. The transition to the B -driven regime occurs at $|B| \sim 50$ mT [Figs. 3(a) and 3(c)], which corresponds to $R_C \approx 1.7 \mu\text{m}$.¹⁴ This length scale is consistent with that found for acoustic-phonon-based interaction between the coplanar 2DESs.⁹ Such a small length scale supports the interpretation in terms of ballistic skipping orbits. In contrast, a qualitatively similar classical picture of hot spots in a 2DES in strong B would give a typical scale at least an order of magnitude larger.¹⁵

The lowest order linear behavior $\delta I_{\text{DET}}, \delta g \propto B$ in Figs. 3(a) and 3(c) indicates that breaking of the time-reversal symmetry in magnetic fields is important, which is indeed the case for chiral transport via skipping orbits. The same is true, e.g., for the Hall effect or transverse thermopower [Nernst-Ettingshausen (NE) effect]. In fact, the data of Fig. 3(a) resembles the behavior of the NE coefficient in a bulk 2DES in perpendicular fields.¹⁶ The similarity suggests that the energy flow from the drive circuit is analogous to a temperature gradient. Still, there is an important difference between the experiments. The NE effect comes from the energy dependence of the momentum relaxation time (diffusion contribution) and asymmetry in electron-phonon interaction (phonon drag contribution).¹⁶ In our case, the key ingredient is likely to be the energy dependence of the detector QPC transparency.¹¹

Next, we briefly outline the results for the drive QPC tuned near pinch-off (and the same settings for the detector QPC). Figure 4(d) shows the derivative g plotted versus the drive QPC gate voltage near its pinch-off for three B -field values. At $B=0$, the counterflow is observed and g exhibits a pronounced extremum. The absolute value is nearly two orders of magnitude larger compared to the open regime [Fig. 3(c)], as reported earlier.^{6,11} Figure 4(d) shows that an application of a moderate $|B| \sim 0.5$ T drastically suppresses the signal. The B -dependence is plotted in Fig. 4(a) for two values of V_{DRIVE} [here, the gate voltage is tuned to the $B=0$ extremum in Fig. 4(d)]. Near zero field, the detector signal is roughly even in B and no steep B -dependence is observed, in sharp contrast to the case of open drive QPC

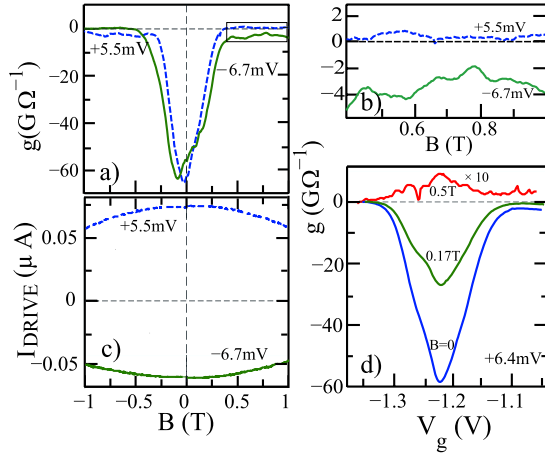


FIG. 4. (Color online) Regime of the nearly pinched-off drive QPC, sample 2, bath temperature of 40 mK. [(a) and (c)] Derivative g of the detector signal for two values of V_{DRIVE} as a function of B and the corresponding traces for I_{DRIVE} . (b) Blown-up $B > 0$ region of (a), where a B -driven behavior is seen, similar to Fig. 3(c). (d) Derivative g of the detector signal at fixed V_{DRIVE} and several values of B as a function of the gate voltage, controlling the drive QPC transparency. In (a)–(c) the linear-response resistance of the drive QPC is $R_{\text{DRIVE}} \sim 80$ k Ω .

[Fig. 3(c)]. Transition to the B -driven regime is found only for $|B| \gtrsim 0.5$ T [Figs. 4(a), 4(b), and 4(d)] with the detector signal comparable to the case of open drive QPC. Note that the impact of the e - h asymmetry discussed above is much stronger in Fig. 4(b) than in Fig. 3(c), which is a result of hot- e injection across the drive QPC near pinch-off.¹⁷ As shown in Fig. 4(c), all these observations are accompanied by a small B -dependence of I_{DRIVE} . The enhanced driving

efficiency for the almost pinched-off drive QPC and its low- B behavior is hard to ascribe to the phonon emission deep in the 2DES leads, unlike for the open drive QPC. Possibly, the energy relaxation of hot e close ($\ll 1$ μm) to a pinched-off QPC is relevant here. Although this is consistent with experiments on transverse focusing of hot e ,¹⁸ we failed to understand the gate voltage and B -field dependencies.⁶

The above discussed phononic effects can be considered as quite general to coupled nanocircuits in magnetic field. The conditions of the present experiment (a relatively small B and a strongly nonlinear regime) are different from those of, say, Refs. 2, 4 and 19, preventing a direct comparison. Still, we find it surprising that the acoustic-phonon-based interaction have not been carefully ruled out in those experiments.

In summary, we have explored the influence of a perpendicular B on acoustic-phonon-based interaction between coplanar nanocircuits in a 2DES. The primary effect of the B is to modify the motion of nonequilibrium carriers in the 2DES leads from a ballistic bulk transport to a skipping-orbit edge transport. As a result, a new B -driven regime is found in moderate B , where a spatial asymmetry of phonon emission/reabsorption is determined solely by field polarity. The observations suggest a possible way to verify the importance of the 2DES related effects in some drag-type experiments.

We acknowledge discussions with R. V. Parfen'ev, D. Bagretz, A. Kamenev, D. V. Shovkun, V. T. Dolgoplov, A. A. Shashkin, A. A. Zhukov, E. V. Deviatov, and R. Fletcher. Financial support by FRBR, RF President Fund under Grant No. MK-3470.2009.2, and the German Excellence Initiative via the "Nanosystems Initiative Munich (NIM)" is gratefully acknowledged. V.S.K. acknowledges support from the Humboldt Foundation and the Russian Science Support Foundation.

- ¹P. Debray *et al.*, *J. Phys.: Condens. Matter* **13**, 3389 (2001); P. Debray *et al.*, *Semicond. Sci. Technol.* **17**, R21 (2002).
- ²M. Yamamoto *et al.*, *Science* **313**, 204 (2006).
- ³R. Aguado and L. P. Kouwenhoven, *Phys. Rev. Lett.* **84**, 1986 (2000).
- ⁴E. Onac, F. Balestro, L. H. Willems van Beveren, U. Hartmann, Y. V. Nazarov, and L. P. Kouwenhoven, *Phys. Rev. Lett.* **96**, 176601 (2006).
- ⁵S. Gustavsson, M. Studer, R. Leturcq, T. Ihn, K. Ensslin, D. C. Driscoll, and A. C. Gossard, *Phys. Rev. Lett.* **99**, 206804 (2007).
- ⁶V. S. Khrapai, S. Ludwig, J. P. Kotthaus, H. P. Tranitz, and W. Wegscheider, *Phys. Rev. Lett.* **97**, 176803 (2006); V. S. Khrapai *et al.*, *Physica E* **40**, 995 (2008); V. S. Khrapai *et al.*, *J. Phys.: Condens. Matter* **20**, 454205 (2008).
- ⁷A. Levchenko and A. Kamenev, *Phys. Rev. Lett.* **101**, 216806 (2008).
- ⁸U. Gasser, S. Gustavsson, B. Küng, K. Ensslin, T. Ihn, D. C. Driscoll, and A. C. Gossard, *Phys. Rev. B* **79**, 035303 (2009).
- ⁹G. J. Schinner, H. P. Tranitz, W. Wegscheider, J. P. Kotthaus, and S. Ludwig, *Phys. Rev. Lett.* **102**, 186801 (2009).

- ¹⁰D. Harbusch, D. Taubert, H. P. Tranitz, W. Wegscheider, and S. Ludwig, *Phys. Rev. Lett.* **104**, 196801 (2010).
- ¹¹V. S. Khrapai, S. Ludwig, J. P. Kotthaus, H. P. Tranitz, and W. Wegscheider, *Phys. Rev. Lett.* **99**, 096803 (2007).
- ¹²U. Gasser, S. Gustavsson, B. Küng, K. Ensslin, and T. Ihn, *Nanotechnology* **21**, 274003 (2010).
- ¹³H. A. Fertig and B. I. Halperin, *Phys. Rev. B* **36**, 7969 (1987).
- ¹⁴A length scale estimate is quite rough, as follows from a factor of 2 different B scales of the linear regions in Figs. 3(a) and 3(c) near zero magnetic field. The origin of the discrepancy was not studied.
- ¹⁵U. Klöß, W. Dietsche, K. von Klitzing, and K. Ploog, *Z. Phys. B: Condens. Matter* **82**, 351 (1991).
- ¹⁶R. Fletcher, *Semicond. Sci. Technol.* **14**, R1 (1999).
- ¹⁷A. Palevski, M. Heiblum, C. P. Umbach, C. M. Knoedler, A. N. Broers, and R. H. Koch, *Phys. Rev. Lett.* **62**, 1776 (1989).
- ¹⁸J. G. Williamson, H. van Houten, C. W. J. Beenakker, M. E. I. Broekaart, L. I. A. Spendeler, B. J. van Wees, and C. T. Foxon, *Surf. Sci.* **229**, 303 (1990).
- ¹⁹D. Sprinzak, E. Buks, M. Heiblum, and H. Shtrikman, *Phys. Rev. Lett.* **84**, 5820 (2000).